https://doi.org/10.18321/ectj1032

Powder Composition Structurization of the Ti-25Al-25Nb (at.%) System upon Mechanical Activation and Subsequent Spark Plasma Sintering

Ye.A. Kozhakhmetov[1]*, M.K. Skakov[2], Sh.R. Kurbanbekov[3], N.M. Mukhamedov[4], N.Ye. Mukhamedov[4]

[1]D. Serikbayev East Kazakhstan Technical University, 69 Protozanov str., Ust-Kamenogorsk, Kazakhstan
[2]National Nuclear Center of the Republic of Kazakhstan, 2 Beybit Atom str., Kurchatov, Kazakhstan
[3]H.A. Yassawi International Kazakh-Turkish University, 29 Bekzat Sattarkhanov ave., Turkistan, Kazakhstan
[4]Institute of Atomic Energy Branch of the National Nuclear Center of the Republic of Kazakhstan, 10 Beybit Atom str., Kurchatov, Kazakhstan

Article info

Received:
5 October 2020

Received in revised form:
28 November 2020

Accepted:
16 January 2021

Keywords:
Ti-Al-Nb system
Mechanical activation
Spark plasma sintering (SPS)
Microstructure
Composite particles

Abstract

The results of a study of the microstructure evolution of pre-mechanically activated elementary powders based on the Ti-25Al-25Nb (at.%) compositions differing in the particle size of the aluminum (Al) component are presented. It was found that during the mechanical activation, most of the Al was dissolved in the Ti and Nb lattices by interpenetration with the formation of solid solutions (Ti, Al) and (Nb, Al). It has been established that an increase in temperature to 1400 °C, when sintering powder materials based on the Ti-Al-Nb system, leads to a sharp increase in the temperature of Al particles, as a result of the melting of which it is impossible to control the phase formation, which ultimately leads to the difficulty of obtaining the required product. It was determined that in the process of spark-plasma sintering of mechanically activated compositions, intermetallic compounds are formed based on phases – α_2, B2 and O, and with an increase in the sintering temperature, their morphology and distribution in the alloy volume change.

1. Introduction

Recently, the issue of using hydrogen as an alternative energy source has been widely considered [1, 2]. The main difficulties in its practical use are issues related to ensuring its safe storage and transportation, which directly depend on the chemical and physical properties of hydrogen [3, 4]. Today titanium aluminides with a high niobium content are considered as one of the promising materials for the storage and transportation of hydrogen since these compounds have a wide range of homogeneity. However, one of the main problems in the development of this area is the lack of a reliable manufacturing technology that could provide the necessary properties for these materials, depending on their purpose [4–8].

Spark plasma sintering (SPS) is one of the effective methods for producing high-quality products from powder compositions. This method makes it possible to form complex coordination compounds and multicomponent compositions of various dispersion with increased operational properties in a small amount of time and one stage [9, 10]. The use of pre-mechanical activation (MA) of reaction mixtures in high-energy mills before SPS allows the formation of a more uniform fine-grained structure of synthesis products with increased content of dissolved elements (above the values of limiting solubility) and activates less thermodynamically preferable reactions, thereby providing the ability to control the phase composition of composite powders [11–14]. In addition, it is known [15] that, during sintering, the boundary diffusion coefficient is determined by the surface layer structure, and not by the refractory core of the particles, as a result of which, after MA of the powder mixture, there is a significant decrease in temperature of their consolidation, grain growth and bridges due to high surface diffusion.

*Corresponding author. E-mail: kozhahmetov_e@nnc.kz

Thus, the use of technological methods for the formation of highly nonequilibrium materials in powder metallurgy of intermetallic compounds (IMC) based on the Ti-Al-Nb system enables creating a new class of materials with the required structure and desired properties. In this regard, in the paper, the possibility of obtaining an IMC by combining technological methods of preliminary MA with subsequent SPS was studied, as well as the evolution of the microstructure and phase composition of material obtained with MA and SPS was determined.

2. Material and research method

The IMC studied in this paper based on the Ti-25Al-25Nb (at.%) system was obtained by combining the MA and IPA methods. As starting materials, titanium powder with a particle size of 45–60 μm, niobium powder with a particle size of 40–63 μm, as well as aluminum powders with a particle size in a wide range (aluminum nanopowder; aluminum powder (50–60 μm); aluminum shavings (100–150 μm)) were used.

Mixing of powders followed by MA was carried out using a P100SM planetary mill at a ratio of masses of 10 mm milling materials to the processed material as 23: 1. To prevent contamination of the powder composition with the material of the grinding bodies in the MA process, grinding bowls with a protective jacket and balls of zirconium oxide were used. Detailed parameters of the MA and SPS are given in Table.

The SPS of the mixtures was carried out on an SPS-515S installation (Syntex Inc., Japan) in vacuum ($5*10^{-2}$ mbar). The change in the linear dimensions of the ceramic material during the sintering was recorded by the built-in means of technological equipment. The temperature during sintering was recorded with a high-temperature pyrometer (measurement temperature range is 575–2500) through a technological orifice in the side wall of the mold. The block diagram of the systematic combination of preliminary MA of a three-component powder mixture and subsequent SPS is shown in Fig. 1.

The morphology and particle size distribution of mechanically activated powders, as well as microstructure and elemental composition of the obtained IMC, were researched in the topographic and compositional contrast mode using a Tescan-Vega3 scanning electron microscope with an energy dispersive spectral analysis attachment. Determination of the particle size distribution after the MA process was carried out using the Altamistudio software package.

X-ray phase analysis (XRD) of the studied mixtures was carried out on an Empyrean multipurpose X-ray diffractometer in Cu-Kα monochromatic radiation using an automation system. The phase composition was deciphered using the HighScore program.

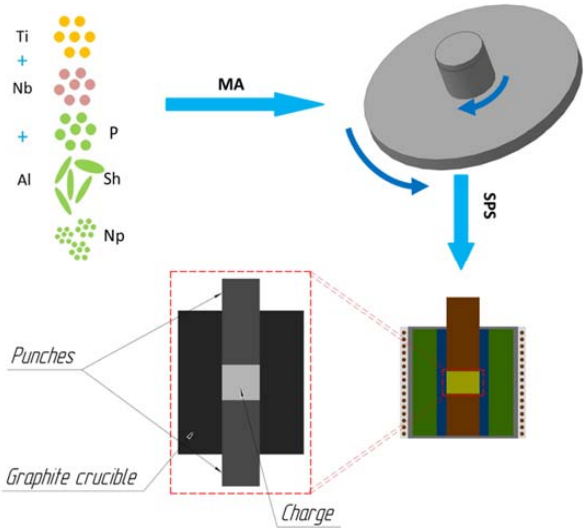

Fig. 1. The block diagram of technological process combination to obtain the IMC system Ti-Al-Nb.

Table

MA parameters

Material	Duration, min	Rotation speed, rpm	Sintering temperature, °C	Exposure, min
Mixing				
Mixture Ti-Al-Nb	35	250	Spark plasma sintering	
MA				
Mixture Ti-Al-Nb (MA-1Sh, shavings) Mixture Ti-Al-Nb (MA-1P, powder) Mixture Ti-Al-Nb (MA-1Np, powder)	20	650	1000 1200	5
Mixture Ti-Al-Nb (MA-2Sh, shavings)	180	350		

3. Results and discussion

3.1. Mechanical activation

The main results on the study of MA parameters influence the morphology and structure formation of composite particles in a mixture based on the Ti-25Al-25Nb (at%) system are given by the authors in [16, 17].

In particular, it was shown in [16] that during MA, most of Al was dissolved in the Ti and Nb lattices by interpenetration with the formation of solid solutions (Ti, Al) and (Nb, Al). Thus, during MA, as a result multiple effects of "cold welding" Al, Ti, Nb are destroyed and formed into layered composite particles. However, in the case of the MA-1Np mixture with the use of aluminum nanopowder, after treatment for 20 min, aluminum "adhered" to titanium and niobium particles without the formation of a solid solution (Fig. 2). After MA, produced composite particles were characterized by high inhomogeneity and had a multifaceted shape.

Analysis of the particle size after MA showed that the distribution of particles is uneven throughout the volume of mixtures (Fig. 3). This distribution is due to the multiple plastic deformations of particles, their cyclic conglomerations and destruction, as a result of which, after MA, the proportion of both small and large fractions increases [18–20]. The most susceptible to the conglomeration of particles powder mixed with aluminum shavings MA-1Sh and MA-2Sh and a particle size greater than 100 μm, wherein the mixture with the use of aluminum powder and nano-powder fraction with a size greater than 300 μm were not be identified. Thus, it can be concluded that the conglomeration of particles depends on the duration of the MA process, since with an increase in the MA time, constant

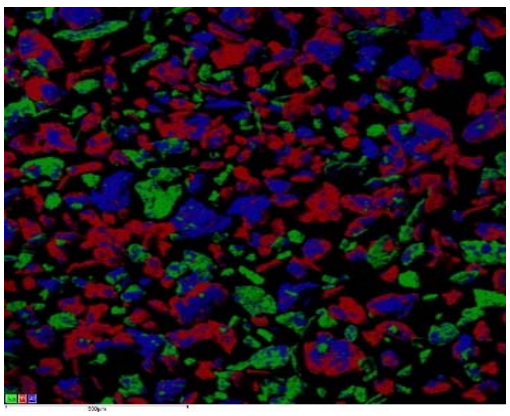

Fig. 2. MA-1Np powder mixture overlay maps after MA (Ti-red, Al-blue, Nb-green).

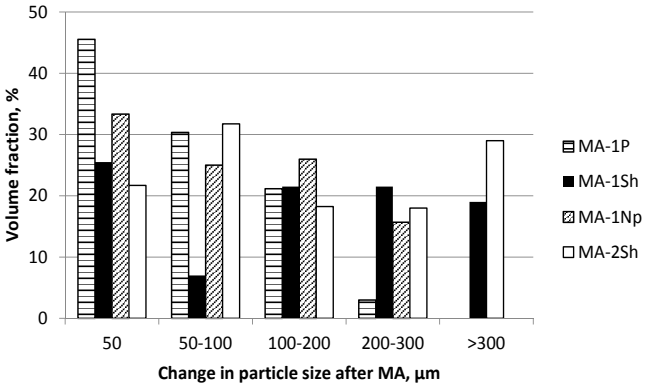

Fig. 3. Particle size distribution after MA.

activation of the particle surface occurs, which in turn leads to the "cold welding" of particles. According to the authors of [21], as the MA time increases, the particle size in the powder mixture continuously decreases to nanometer-sized with the formation of various phases, similar to the intermetallic B2 and O phases. At the same time, the atmosphere of the MA process plays an important role, since the nominal atmosphere affected the time required for the formation of different phases and also the final constitution of the powder.

3.2. Spark plasma sintering

Primary experiments were carried out at a temperature of 1500 °C, static pre-pressing pressure of 60 MPa, a heating rate of 100 °C/min, and an isothermal holding time for 15 min. In the produced samples, melting of the aluminum component of the mixture was observed, which hurt the quality of products. In this regard, further experiments were carried out at temperatures of 1000–1300 °C, static pre-pressing pressure of 20 MPa and isothermal holding for 5 min.

Figure 4 shows the curve of the change in the linear dimensions of Ti-Al-Nb samples in the course of electro-pulse plasma sintering up to a temperature of 1200 °C, analysis of which has made it possible to set the following features during the consolidation of the test material. The shrinkage curves of the samples are of two stages. High intensity of thermal shrinking under pressure of 20 MPa is a country with relatively low temperatures (below the sensitivity limit of the pyrometer) and proceeds to temperatures up to 635–685 °C (depending on the type of powder), its intensity with approaching the temperature of 575 °C, increases. Within the temperature range of 635–840 °C (depending on the

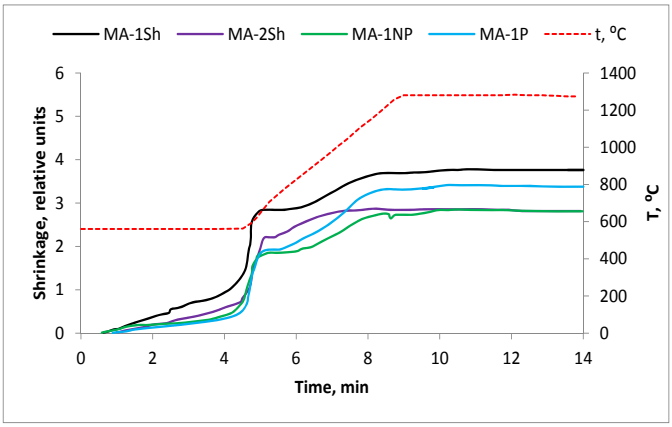

Fig. 4. Dynamics of linear shrinkage of reaction mixtures based on Ti-Al-Nb in the course of electro-pulse plasma sintering at a temperature of 1200 °C.

type of powder), shrinkage almost stops. For MA-1 (P) and MA-2 (Sh) powders, the period of slow shrinkage is too short, which can be explained by melting and uniform distribution in the volume of the aluminum component of the powder mixture. A further increase in temperature to 1100–1200 °C (depending on the type of powder) is accompanied by significant shrinkage. It should be noted that the main share of shrinkage falls on the non-isothermal stage of heating, which indicates a high intensity of material consolidation.

3.3. Microstructural studies of the IMC of the Ti-Al-Nb system obtained by combining MA and SPS

Figure 5 shows the XRD study results of samples obtained by combining MA and subsequent SPS at 1000 °C. Sintering temperatures were selected experimentally and depending on the phase diagram of the Ti-Al-Nb ternary system. According to the XRD results for all samples (Fig. 5a), three main phases α_2, $AlNb_2$, and B2 were observed at a relatively low sintering temperature (1000 °C), and relatively low content of the O-phase was also found. In this case, in diffraction patterns of the MA-2Sh and MA-1Np samples, the peaks of the O-phase are have higher intensity, whereas for the other two samples (MA-1Sh, MA-1P), the reverse pattern emerged. Samples sintered at 1000 °C are characterized by a volumetric amount of unreacted Nb. However, the Nb content, the same as with O-phase, depends on the time of the MA process and aluminum component size of the initial burden. The highest (Fig. 5b) content of unreacted Nb is typical for samples with aluminum shavings in the initial composition, where, as a result of MA, the conglomeration of particles with a size of more

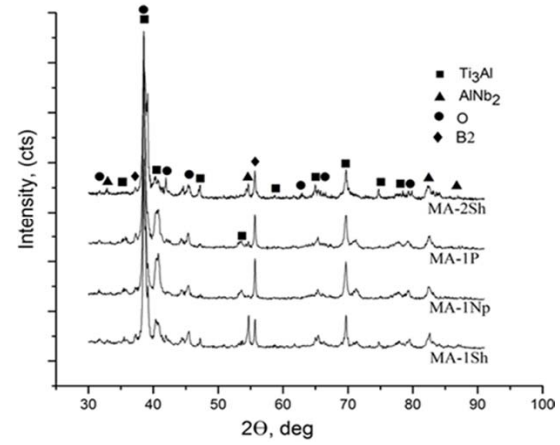

(a)

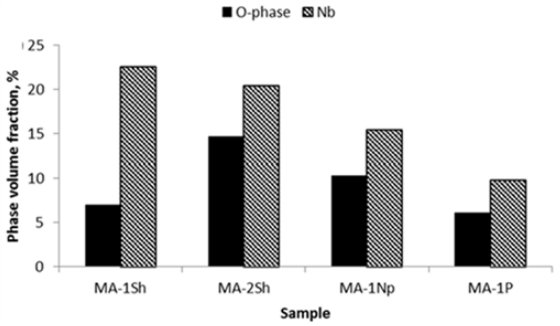

(b)

Fig. 5. The XRD results of samples sintered at 1000 °C/5 min/20 MPa: (a) – diffraction pattern; (b) – phase distribution.

than 300 μm was observed. At the same time with MA-2Sh sample increased content of the O-phase was also found in comparison with other samples. Increasing the length of time MA leads to improved fluidity of mixed powders, which in turn has a positive effect on the formation of the O-phase [22].

All samples sintered at 1000 °C are characterized by an inhomogeneous multiphase structure (intermetallic α_2, $AlNb_2$, B2, O phases) without pores and cracks with massive secretions of unreacted niobium. Figure 6 shows images of the heterogeneous structure surface of the samples sintered at 1000 °C in the composite shooting mode, obtained using SEM.

The increase in sintering temperature to 1200 °C in all samples led to a noticeable decrease in the structural heterogeneity of the obtained materials. According to the results of XRD for the samples, increased content of the B2-phase is observed, while (Fig. 7b) the volume fraction of the -α_2 phase has significantly decreased. Thus, samples sintered at both 1000 °C and 1200 °C are characterized by an increased content of the B2 phase (Fig. 7b).

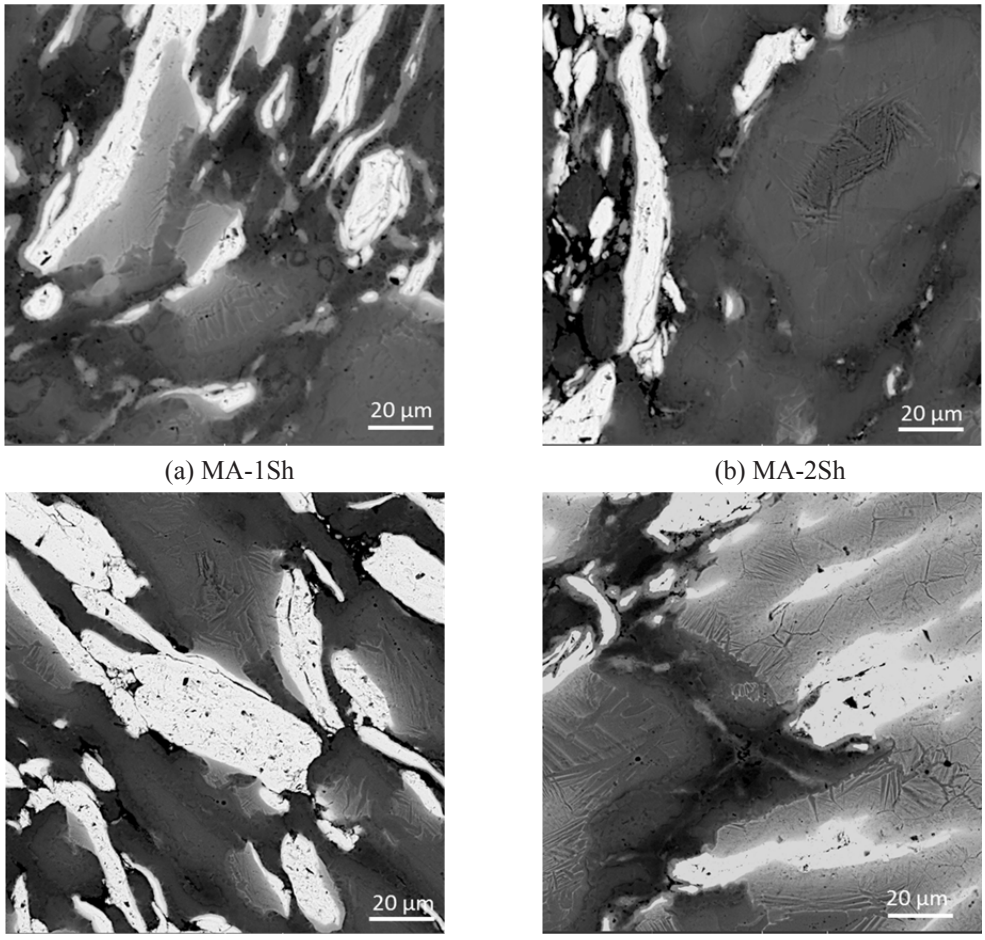

(a) MA-1Sh (b) MA-2Sh

(c) MA-1Np (d) MA-1P

Fig. 6. SEM image of samples of the Ti-25Al-25Nb (at%) system sintered at 1000 °C/5min/20 MPa.

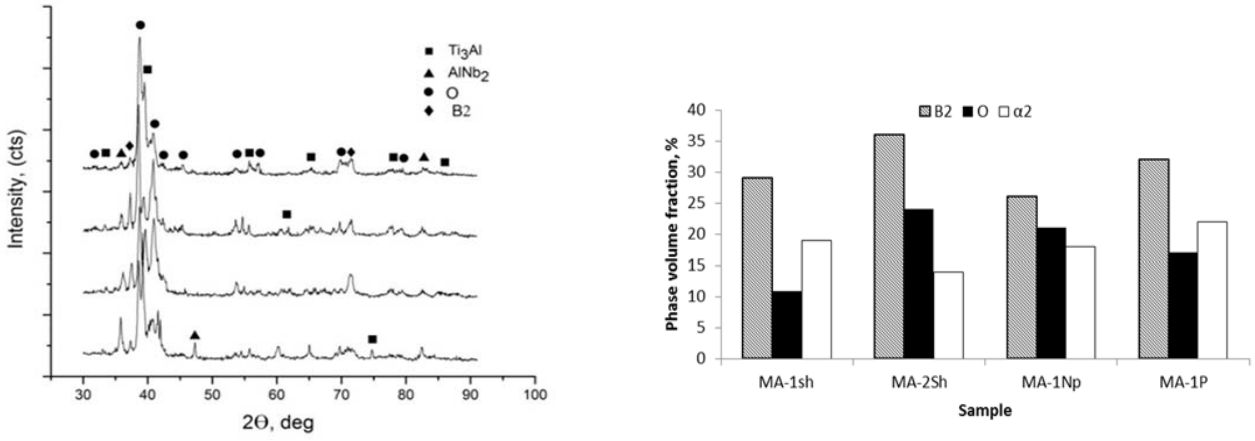

(a) (b)

Fig. 7. The XRD results of samples sintered at 1200°C/5 min/20 MPa: (a) – diffraction pattern; (b) – phase distribution.

According to the authors of [23, 24], during SPS in dynamics of linear shrinkage of reaction mixtures based on Ti-Al-Nb at a temperature of 1200 °C, two endothermic peaks are observed in the temperature range of 850–1150 °C, which, according to the Ti-22Al-Nb phase diagram [24], corresponds to the IMC phase transformation Ti_2AlNb. S.L. Semiatin and others assume that the first peak corresponds to the transition of the α_2 + B2/β + O phases to the α_2 + B2 phase, while the second peak corresponds to the transition of the α_2 + B2 phase to the B2 phase, which explains increased content of the B2 phase in all samples obtained both at the sintering temperature of 1000 °C and 1200 °C. In our case, during the consolidation of elementary powders after MA, we observed a similar two-stage

dynamics of linear shrinkage of the sintered samples (Fig. 4). However, temperature boundaries of the phase transformations of the IMC were smaller and took place in the range of 575–850 °C. This may be due to preliminary MA, which had a beneficial effect on the subsequent consolidation of elemental powders. It should be considered that the compositions studied in this work have a higher content of aluminum, and this can shift the boundaries of phase transformations very much.

In the microstructure of the obtained samples, regardless of aluminum component particle size, individual grains of the B2 phase was found, where the formation of the Widmannstatten structure was observed. In addition, in the samples obtained from mechanically activated powders for 20 min (MA-1Sh, MA-1Np and MA-1P), in addition to the O-phase, a small amount of the α_2-phase and the $AlNb_2$ phase was observed.

An increase in the sintering temperature leads to significant changes in the size and distribution of the O-phase. This phase has become larger and lamellar in a structure of 10 μm thick and up to 50 μm long and is mainly concentrated in the body of B2 grains. This can be explained by the fact that higher temperature provides more active energy for the diffusion process, which accelerates the growth of the O-phase lamellar shell. Another feature of the O-phase at a given temperature is its distribution at the B2/α_2 interface, which plays the role of a diffusion barrier between the α_2 and B2 phases, limiting the growth of the size of these phases.

It should be noted that the $AlNb_2$ phase distribution on the surface of all samples at the sintering temperature of 1200 °C has clear boundaries and is dispersed around the inclusions of unreacted niobium, enveloping them. However, when studying the microstructure of samples of MA-1Np and MA-1P powder mixture, an accumulation of this phase is observed in the form of short needle-like inclusions up to 2–3 μm thick and 10–15 μm long, distributed over the entire grain boundary of the B2 phase, and in some cases in the grain body of B2 phase (Figs. 8c, d).

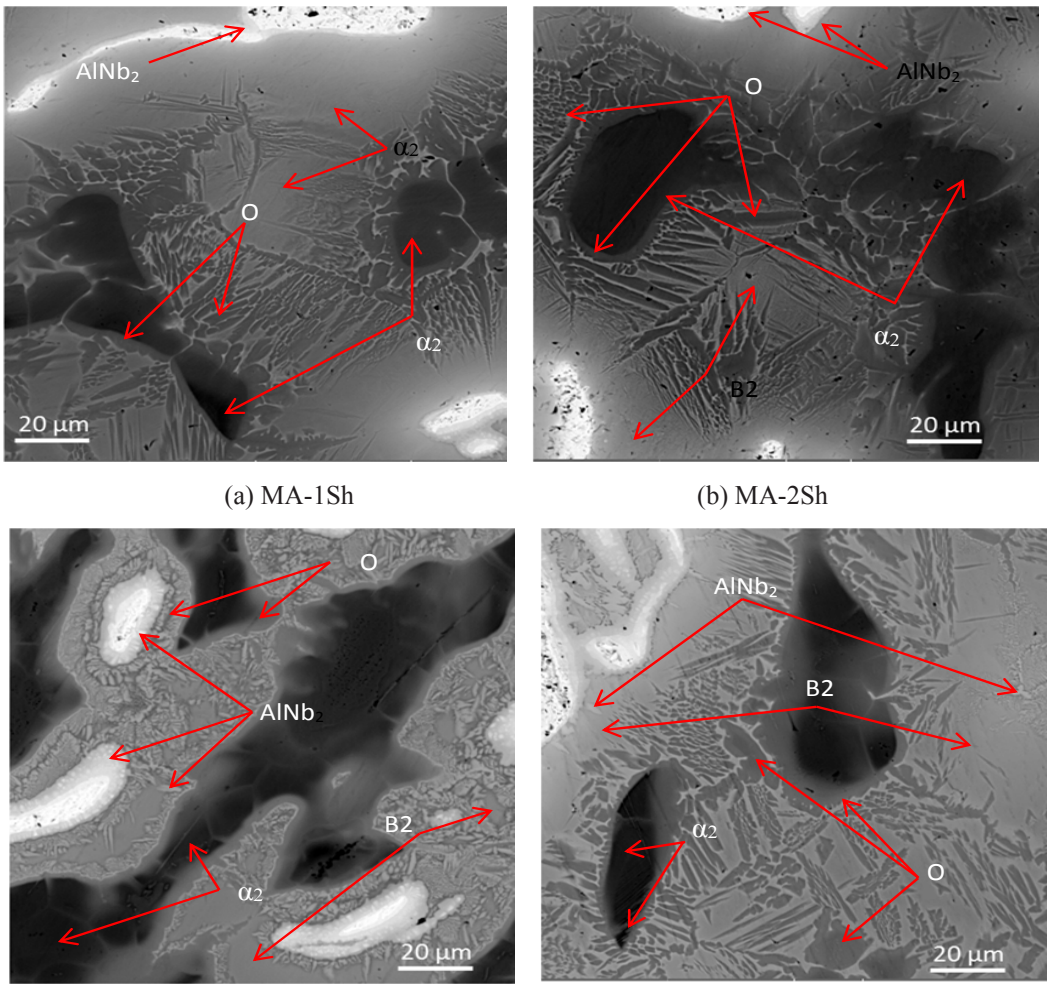

(a) MA-1Sh (b) MA-2Sh

(c) MA-1Np (d) MA-1P

Fig. 8. SEM-images of the samples Ti–25Al–25Nb (at %) system sintered at 1200 °C/5 min/20 MPa.

According to the results of electron microscopic studies, well seen that the distribution and morphology of the O-phase have many facets, which depends to a greater extent on the size of Al particles in the initial burden and the modes of the preliminary MA and as shown in Fig. 8. For example, for MA-2Sh, MA-1P and MA-1Np samples, the presence of a wide lamellar structure of the O-phase with a size of fewer than 8 μm in the grain body of the B2 phase is inherent. As shown in Figs. 8c, b and d by the whole grain boundary phase B2 and α_2 are observed aligned long strap O-phase which create a potential barrier between the base B2 and α_2-phase. At the same time, in the MA-2 Sh and MA-2P samples, the presence of 2–3 μm globular accumulations of the O-phase in the body of the B2-phase grain was recorded, while in the MA-2P sample, the presence of a round-shaped O-phase with an average diameter of 18 μm was detected. In this case, along the boundaries of this O-phase, a change in the stoichiometric composition was found, where a continuous section depleted in niobium is observed. Y. He and others [25] explain this effect in the samples by the decomposition of the metastable B2 phase into the α_2 and/or O phase as a result of multiple transformations during sintering and subsequent cooling in the furnace. A feature of the distribution of the O-phase in the sample with aluminum shavings in the initial burden and mechanically activated for 20 min (MA-1Sh) is the presence of thin continuous veinlets of the O-phase along the entire boundary of needle inclusions of the $AlNb_2$-phase.

As evidenced in Fig. 7b, the highest O-phase content of 39% was recorded in the MA-2Sh sample, which was activated for 180 min. However, it is necessary to pay attention to the fact that the large size of particles in the initial mixture and their conglomeration during MA negatively affects the O-phase fraction in the sample volume and reduces it. This is well illustrated in the MA-1Sh sample, where the lowest content of the O-phase and the highest content of the α_2-phase were recorded.

4. Conclusion

According to the results of experimental work to study the evolution of the particle structure of a metal powder mixture based on the Ti-Al-Nb system of preliminary MA and subsequent SPS, the following conclusions can be drawn:

1. During MA, most of Al dissolves in the Ti and Nb lattices by interpenetration with the formation of (Ti, Al) and (Nb, Al) solid solutions. Thus, at the time MA, as a result of multiple effects of "cold welding" of Al, Ti, Nb and destruction of layered composite particles are formed, the size of which depends on the duration of the MA process. With an increase in the MA time, constant activation of the particle surface occurs, which in turn leads to the "cold welding" of particles (to the conglomeration of particles).

2. An increase of the temperature to 1400 °C, when sintering powder materials based on the Ti-Al-Nb system, leads to a sharp increase in the temperature of Al particles in the mixture. Due to particle melting, it is impossible to control the phase formation, which ultimately leads to the complexity of obtaining the desired product. Based on the results of the work, it can be concluded that the search for optimal modes of electric pulse plasma sintering for powder mixtures of MA-1 (Sh), MA-1 (Np), MA-1 (P) and MA-2 (Sh) should be carried out in the temperature range of 850–1200 °C with heating rates of 150–200 °C/min, which will minimize the risk of melting of the aluminum component during high-temperature consolidation.

3. All samples sintered at 1000 °C are characterized by a non-uniform multiphase structure (intermetallic α_2, $AlNb_2$, B2, O phases) without pores and cracks with massive secretions of unreacted niobium.

4. An increase in the sintering temperature to 1200 °C in all samples leads to a noticeable decrease in the heterogeneity of structure of the obtained materials. The main surface matrix for these samples is the B2 phase.

5. The distribution and morphology of the O-phase have a versatile character, which depends to a greater extent on the size of Al particles in the initial burden and the preliminary MA modes. Thus, for MA-2Sh, MA-1P and MA-1Np samples, the presence of a wide lamellar structure of the O-phase in the body of B2 phase grains is inherent. While the presence of globular accumulations of the O-phase was recorded on the MA-2Sh and MA-2P samples.

Acknowledgments

The work was carried out as part of the scientific and technical program "Development of nuclear power in the Republic of Kazakhstan for 2018–2020" on the topic "Research of promising materials based on the Ti-Al-Nb system for storage and transportation of hydrogen".

References

[1]. A. Pareek, R. Dom, J. Gupta, J. Chandran, V. Adepu, P.H. Borse, *Mater. Sci. Energy Technol.* 3 (2020) 319–327. DOI: 10.1016/j.mset.2019.12.002

[2]. J.O. Abe, A.P.I. Popoola, E. Ajenifuja, O.M. Popoola, *Int. J. Hydrogen Energ.* 44 (2019) 15072–15086. DOI: 10.1016/j.ijhydene.2019.04.068

[3]. E. Boateng, A. Chen, *Materials Today* Advances 6 (2020) 2–11. DOI: 10.1016/j.mtadv.2019.100022

[4]. M. Nagpa, R. Kakkar, *Int. J. Hydrogen Energ.* 43 (2018) 12168–12188. DOI: 10.1016/j.ijhydene.2018.04.103

[5]. Sh. Kurbanbekov, M. Skakov, V. Baklanov B. Karakozov, *Mater. Test.* 59 (2017) 1033–1036. DOI: 10.3139/120.111107

[6]. J. Coleto, J. Goni, P. Egizabal, M. García de Cortázar, G. Lilly, X. Sainz, L. Pambaguian, *Materials Science Forum* 426-432 (2003) 2145–2150. DOI: 10.4028/www.scientific.net/MSF.426-432.2145

[7]. J. Shen, A. Feng, *Acta Metall. Sin.* 49 (2013) 1286–1294. DOI: 10.3724/SP.J.1037.2013.00607

[8]. Y. Huang, Y. Liu, C. Li, Z. Ma, L. Yu, H. Li, *Vacuum* (2019) 209–219. DOI: 10.1016/j.vacuum.2018.12.044

[9]. H. Fang, R. Chen, X. Chen, Y. Yang, Y. Su, H. Ding, J. Guo, *Intermetallics* 104 (2019) 43–51. DOI: 10.1016/j.intermet.2018.10.017

[10]. I. Polozov, V. Sufiiarov, A. Kantyukov, N. Razumov, I. Goncharov, T. Makhmutov, A. Silin, A. Kim, K. Starikov, A. Shamshurin, A. Popovich, *Addit. Manuf.* 34 (2020) 1–14. DOI: 10.1016/j.addma.2020.101374

[11]. W. Wang, H. Zhou, Q. Wang, Y. Gao, K. Wang, *J. Mater. Eng. Perform*. 29 (2020) 1686–1695. DOI: 10.1007/s11665-020-04610-6

[12]. K-H. Sim, G. Wang, J-M. Ju, J. Yang, X. Li, *J. Alloy. Compd.* 704 (2017) 425–433. DOI: 10.1016/j.jallcom.2017.01.354

[13]. A. Kaliyeva, Y. Tileuberdi, L. Galfetti, Y. Ongarbayev, *Eurasian Chem.-Technol. J.* 22 (2020) 141–147. DOI: 10.18321/ectj962

[14]. E. Kozhahmetov, B. Karakozov, S. Kurbanbekov, *Key Eng. Mater.* 743 (2017) 41–44. DOI: 10.4028/www.scientific.net/kem.743.41

[15]. K.S. Senkevich, M.M. Serov, O.Z. Umarova, *Met. Sci. Heat Treat.* 59 (2017) 66–69. DOI: 10.1007/s11041-017-0172-3

[16]. Ye. Kozhakhmetov, M. Skakov, W. Wieleba, Sh. Kurbanbekov, N. Mukhamedova, *AIMS Materials Science* 7 (2020) 182–191. DOI: 10.3934/matersci.2020.2.182

[17]. Ye. Kozhakhmetov, M. Skakov, N. Mukhamedova, Sh. Kurbanbekov, Sh. Ramankulov, W. Wieleba, *Mater. Test.* 63 (2021) 119–123. DOI:10.1515/mt-2020-0017

[18]. J. Jia, W. Sun, W. Peng, Z. Yang, Y. Xu, X. Zhong, W. Liu, J. Luo, *Adv. Powder Technol.* 3 (2020) 1963–1974. DOI: 10.1016/j.apt.2020.02.029

[19]. O. Kaipoldayev, Ye. Mukhametkarimov, R. Nemkaeva, G. Baigarinova, M. Aitzhanov, A. Muradov, N. Guseinov, *Eurasian Chem.-Technol. J.* 19 (2017) 197–200. DOI:10.18321/ectj194

[20]. C.J. Boehlert, B.S. Majumdar, V. Seetharaman, D.B. Miracle, *Metall. Mater. Trans. A* 279 (2000) 118–129. DOI: 10.1007/s11661-999-0240-4

[21]. G.-H. Chen, C. Suryanarayana, F.H.S. Froes, *Metall. Mater. Trans. A* 26 (1995) 1379–1387. DOI: 10.1007/BF02647588

[22]. G. Wang, J. Yang, X. Jiao, *Mat. Sci. Eng. A-Struct.* 654 (2016) 69–76. DOI: 10.1016/j.msea.2015.12.037

[23]. J. Kundu, A. Chakraborty, S. Kundu, *Weld. World* 64 (2020) 2129–2143. DOI: 10.1007/s40194-020-00989-x

[24]. H. Zhang, N. Yan, H. Liang, Y. Liu, *J. Mater. Sci. Technol*. 80 (2021) 203–216. DOI: 10.1016/j.jmst.2020.11.022

[25]. Y. He, W. Luo, Y. Du, M. Wu, K. Wang, X. Liu, R. Hu, *MATEC Web Conf.* 321 (2020) 11064. DOI: 10.1051/matecconf/202032111064